Design and Synthesis of New Histamine H4 Receptor Ligands

Smits, R.A.

2009

CHAPTER 6

In vivo evaluation of the potent Histamine H_4 receptor ligands [^{11}C]JNJ7777120 and [^{11}C]VUF10558 for monitoring inflammatory processes using PET.

Smits, R., A.[a]; Moojer, M., P., J.[b] de Esch, I., J., P.[a] Zuiderveld, O., P.;[a] Adami, M.;[c] Guaita, E.;[c] Coruzzi, G.;[c] Leurs, R.;[a] Windhorst, A., D.[b]

[a]Leiden/Amsterdam Center for Drug Research (LACDR), Division of Medicinal Chemistry, Department of Pharmacochemistry, Faculty of Exact Sciences, Vrije Universiteit Amsterdam, De Boelelaan 1083, 1081 HV Amsterdam, The Netherlands.
[b]VU University Medical Center, Department of Nuclear Medicine and PET Research, De Boelelaan 1058c, 1081 HV Amsterdam, The Netherlands.
[c]Department of Human Anatomy, Pharmacology and Forensic Medicine, Section of Pharmacology, University of Parma, via Volturno 39, 43100 Parma, Italy.

Abstract

The two potent histamine H_4 receptor ligands 2-(6-chloro-2-(4-methylpiperazin-1-yl)quinazoline-4-amino)-ethanesulfonamide (VUF10558, **1**) and (5-chloro-1*H*-2-yl)(4-methylpiperazin-1-yl)methanone (JNJ7777120, **2**) were selected to be developed into potential radioligands for monitoring inflammatory processes with positron emission tomography (PET). For this, the compounds were successfully labeled with ^{11}C and were obtained in high radiochemical yield and purity. Evaluation of the radioligands *in vivo* in rats showed two distinct distribution profiles. Compound [^{11}C]**1** did not enter the CNS but was only present in the periphery. In contrast, [^{11}C]**2** was found to rapidly enter the CNS and was retained in hippocampus and olfactory bulb tissue, suggesting the presence of H_4R receptors in these brain areas. Due to their different distribution profiles, the two ligands presented in this study are therefore complementary tools to further characterize the H_4R.

Introduction

The human H_4R receptor (hH_4R) that was discovered in 2001 is the latest addition to the histamine receptor subfamily.[1] This subfamily of G protein-coupled receptors (GPCRs) consists of the H_1, H_2, H_3 and H_4 receptors that all have very distinct expression patterns and physiological functions such as vasodilatation, gastric acid secretion and a role in neurotransmission.[2,3,4] The H_4R has been shown to be involved in inflammatory processes and the use of H_4R antagonists in preliminary *in vivo* models has been successful in counteracting the development of inflammation after a variety of stimuli.[5,6,7] Although the H_4R has been detected in a variety of tissues at the mRNA level by RT-PCR on a number of occasions, the overall expression level is relatively low.[8,9,10,11] However, the H_4 receptor has been detected by immunohistochemical staining on monocytes, leukocytes, intraepithelial cells and enterocytes in the gut.[12,13] The expression of functional H_4R has also been shown on human monocytes and neurons in native brain slices from the rat.[12,14] H_4R expression appears to be limited to specific subtypes of cells or specific local conditions in tissues such as an inflammatory process. For example, the upregulation of H_4R expression in diseased tissues has been postulated for rheumatoid arthritis, where the expression level of the H_4R in synovial tissue taken from rheumatoid arthritis patients might be related to disease severity.[8] More convincingly, varying H_4R expression levels have been found for cell types including CD_4+ Th_2 cells, Langerhans dendritic cells and monocyte-derived-dendritic cells before and after immunological stimuli and illustrates the ability of up- or downregulation of H_4R expression under specific pathophysiological conditions.[9] As mentioned previously, the H_4R has been shown to be present on leukocytes.[15] These cells can migrate to sites of inflammation on a massive scale, thereby potentially increasing the H_4R density in the affected tissues.[16] Under the abovementioned conditions, the H_4R might therefore be used as a target to image inflammatory diseases in various stages of development.

A well known and convenient way to perform whole body imaging and monitoring of disease is by Position Emission Tomography (PET).[17] PET is a true molecular imaging technique that allows for dynamic assessment of radioactivity in time and place, as well as the quantification of the amount of radioactivity. In order to develop potential PET ligands for the H_4R, two H_4R ligands (**1** and **2**, Figure 1) were selected for labeling with Carbon-11, a positron emitting isotope with a half life of 20 minutes. The first compound, VUF10558 (2-(6-chloro-2-(4-methylpiperazin-1-yl)quinazoline-4-amino)-ethanesulfonamide (**1**), was selected from a series of recently discovered quinazoline sulfonamides that showed high

affinity for the human H_4R while acting as an inverse agonist in a CRE-β-galactosidase reporter gene assay.[18] Furthermore, this compound has been shown to have potent anti-inflammatory properties in an *in vivo* model of acute inflammation in the rat after subcutaneous administration.[18] The second compound is the reference antagonist JNJ7777120 (**2**) that has been shown to be selective for the human H_4R (hH_4R) over a large number of other biological targets.[6] Although this compound suffers from a relatively short biological half life after i.v. administration ($t_{1/2}$= 0.8 h in the rat)[19] it is considered to be very suitable for use in the timeframes of up to 90 minutes that are needed for PET imaging with ^{11}C.

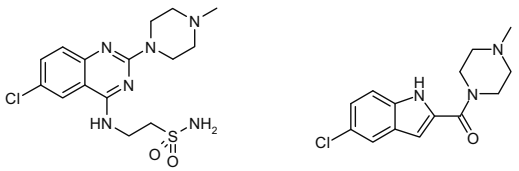

1 **2**

Figure 1: Chemical structures of the hH_4R inverse agonist **1** (VUF10558) and hH_4R antagonist **2** (JNJ7777120).

The most straightforward way to introduce an isotope suitable for PET imaging in both **1** and **2** was methylation of the unsubstituted piperazine precursor of both H_4R ligands with [^{11}C]CH_3I. Using a semi-automated synthetic procedure, the radioligands can be formulated directly after purification and used for immediate *in vivo* imaging experiments to provide new insights into the (patho)physiological role of the H_4R in either naïve animals or in animal models of inflammation. After validation of a radiolabeled compound as a PET tracer *in vivo* in rodents, potential application in humans for disease monitoring or drug development might be feasible.

Chemistry

Preparation of [^{11}C]CH_3I was carried out according to a procedure described in literature[20]. The synthesis of [^{11}C]VUF10558 was started from 2,4,6-trichloroquinazoline (**3**), which was prepared according to a literature procedure (Scheme 1).[21] 2-Aminoethanesulfonamide, prepared according to literature, [22] was coupled selectively to the 4-position of the quinazoline at room temperature after which the 2-position was substituted with Boc-piperazine under microwave assisted heating to give intermediate **4**. Removal of the Boc-group with HCl/dioxane gave the dihydrochloride acid salt of compound **5** that was

subsequently methylated with [^{11}C]CH_3I. After several failed attempts to methylate **5** in MeCN and in the presence of various bases, it was found that a mixture of MeCN/DMF/water (2:3:1) with 5 equivalents of DIPEA gave excellent incorporation of [^{11}C]CH_3 to yield [^{11}C]**1**.

Scheme 1[a]

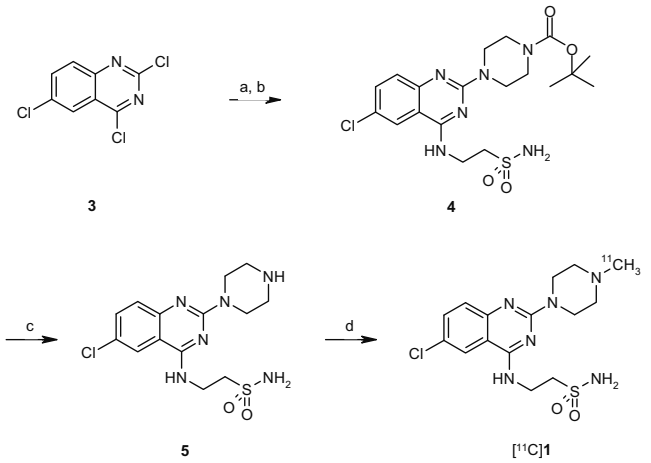

[a]Reagents and conditions: a) $H_2N(CH_2)_2SO_2NH_2$•2HCl, DIPEA, EtOAC, r.t., 20 min; b) boc-piperazine, MW, 140 °C, 10 min (20%, a+b); c) HCl/Dioxane, r.t., 2 h (55%); d) [^{11}C]CH_3I, H_2O/DMF/MeCN, DIPEA, 70 °C, 5 min (40%).

Compound **9** (Scheme 2), the precursor for [^{11}C]**2** was prepared according to a procedure in literature.[23] This precursor was subsequently treated with [^{11}C]CH_3I in MeCN to give the desired radioligand [^{11}C]**2** in good yields.

Scheme 2[a]

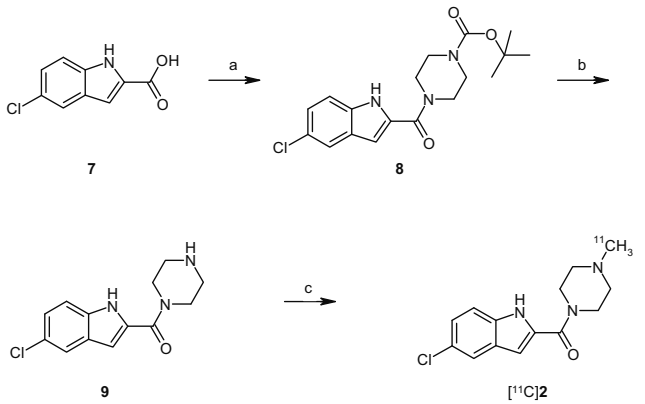

[a]Reagents and conditions: a) CDI, Boc-piperazine, THF, r.t., 16 h (40%); b) HCl/Dioxane, r.t., 16 h (73%); c) [^{11}C]CH_3I, MeCN, DIPEA, 70°C, 5 min (40%).

Results and discussion

Method development for the radiosynthesis of both compounds proceeded smoothly and both tracers were obtained with good reproducibility and yields as well as excellent radiochemical purity (Figure 2). The syntheses were performed with semi-automated procedures allowing direct formulation of the tracers after purification by HPLC (Figures 3 and 4). This reduced the total time for preparation to approximately 45 minutes and furnished the product as an injectable solution in phosphate buffered saline with about 10% EtOH.

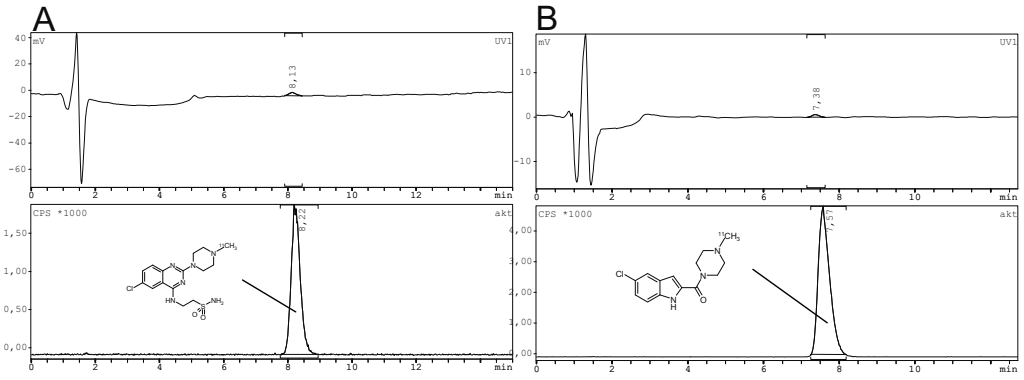

Figure 2: Analytical HPLC analysis of [^{11}C]**1** (A) and [^{11}C]**2** (B) after formulation. The top chromatograms show the UV signal with an injection peak around 1.5 min. Both chromatograms seen in the bottom show the activity signal of the radioligands as a single peak.

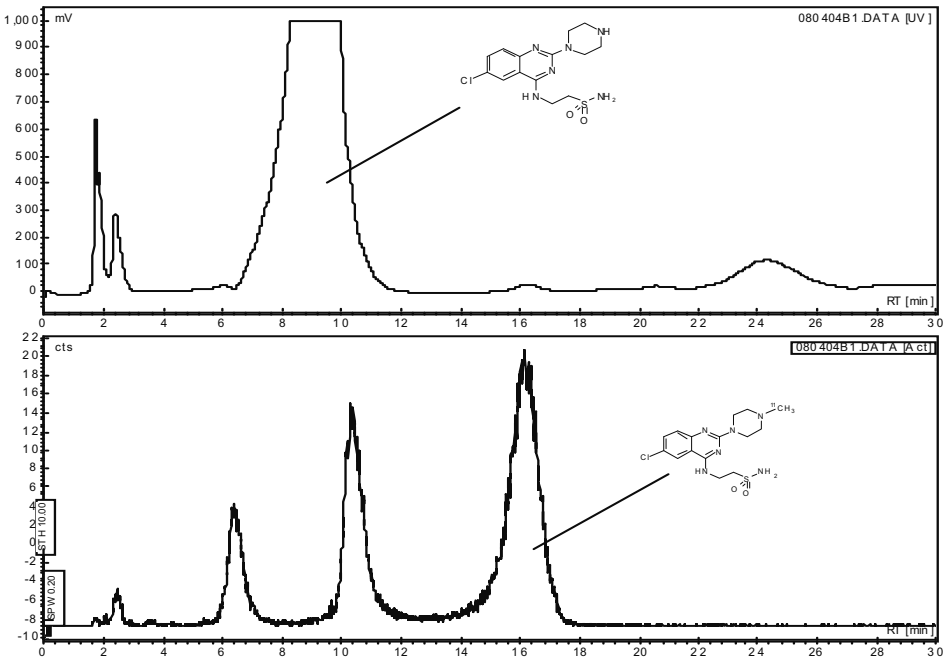

Figure 3: Typical chromatograms of the purification by preparative HPLC of [^{11}C]**1**. The top chromatogram shows the UV signal with a large peak for the unmethylated precursor and a very small product peak around 16 minutes. At the bottom of this figure several activity signals can bee seen with the largest signal for [^{11}C]**1**.

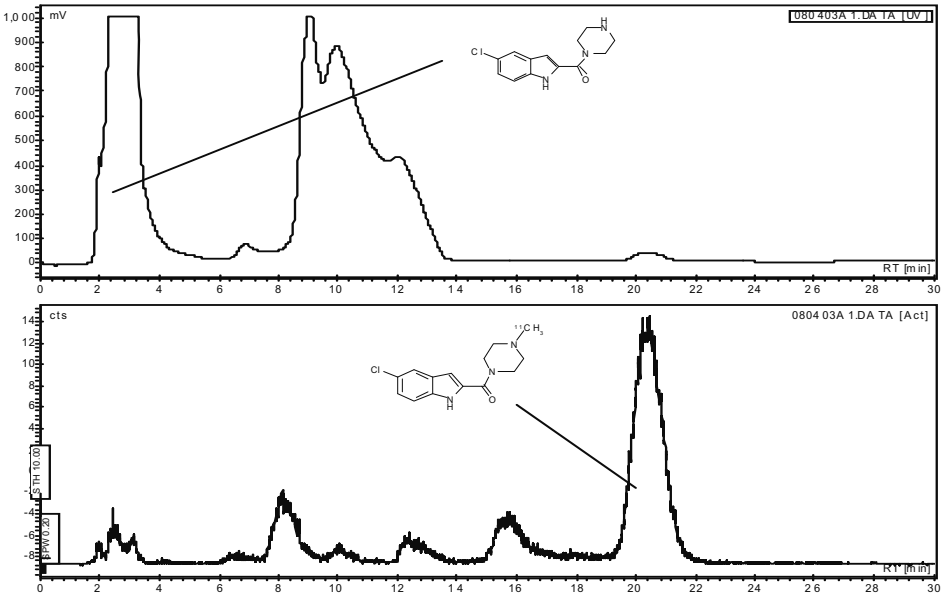

Figure 4: Chromatograms of the purification by preparative HPLC of [^{11}C]**2**. The top chromatogram shows the UV signal with a large peak for the unmethylated precursor and a small product peak around 20 minutes. At the bottom of this figure several activity signals can bee seen with the largest signal for [^{11}C]**2**.

When comparing the biodistribution study of both radioligands in male Wistar rats, a very different distribution profile is observed (Figures 5 and 6). [^{11}C]**1** is mainly found in peripheral organs with high blood throughput but shows very limited uptake in the CNS at all time points (Figure 5). Due to limited uptake in the brain, comparison of uptake between different brain regions could not be performed reliably for this tracer. Compound [^{11}C]**1** is rapidly distributed throughout the sampled tissues and shows only a slow decrease in injected dose per gram over the timeframe of 60 minutes, which suggests a long *in vivo* elimination half life. In comparison, [^{11}C]**2** is distributed even more rapidly (Figure 6). It reaches peak tissue concentrations within 5 minutes after which it is quickly cleared from the body within 60 minutes. This observation is not in exact agreement with the reported *in vivo* half life of 48 minutes of compound **2** and it should be noted that tracer kinetics can be quite different from *in vivo* kinetics of therapeutic doses that are usually much higher, being mg/kg compared to µg/kg dosage in the tracer experiment. The distribution of both compounds over the sampled tissues is relatively low, which might correspond to a low expression of the rH_4R receptor in healthy tissue. The majority of the injected dose of both radioligands is found in the lung, liver

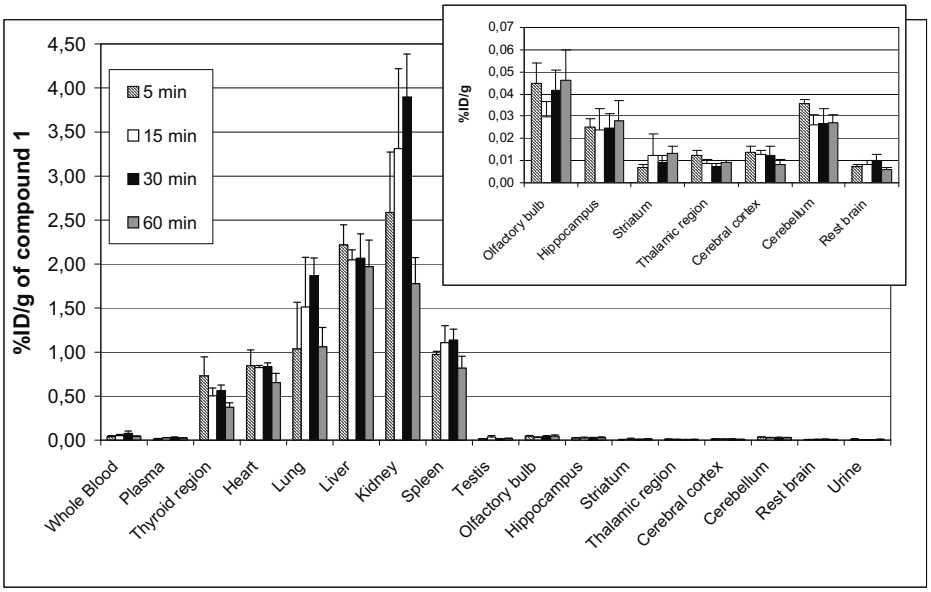

Figure 5: Distribution of [^{11}C]**1** in male Wistar rats measured as percentage injected dose per gram (%ID/g) (n=4). Urine is expressed as %ID. The insert represents a blow-up of the cerebral distribution.

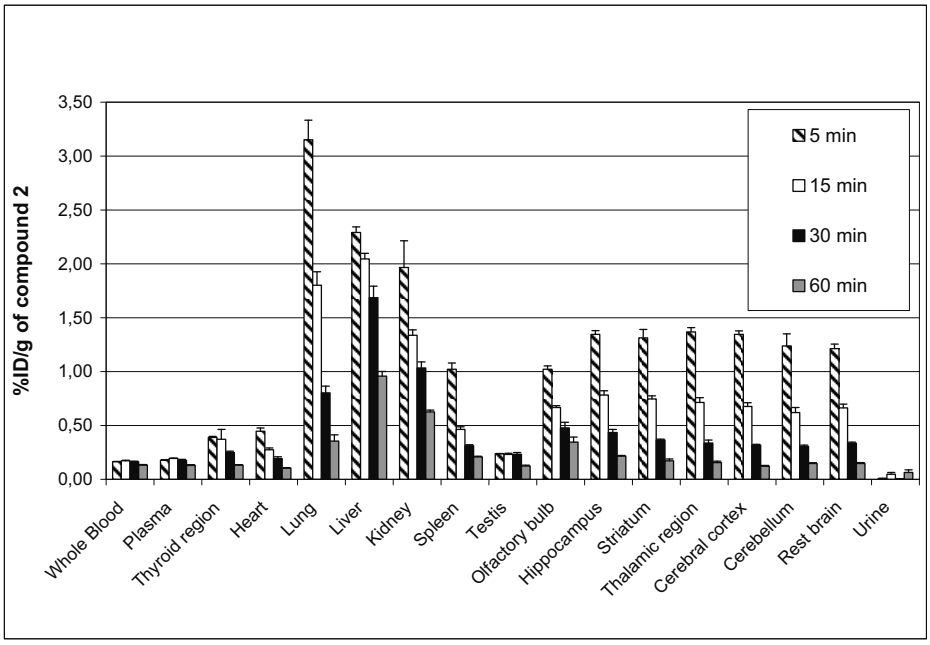

Figure 6: Distribution of [^{11}C]**2** in male Wistar rats measured as percentage injected dose per gram (%ID/g) (n=4). Urine is expressed as %ID.

and kidney and is observed more often for these type of experiments.[24] However, it should be noted that these tissues as well as the spleen have a relatively high content of H_4R mRNA.[9,10,11] Therefore, it can not be excluded that the observed retention is due to H_4R binding in these tissues.

Interestingly, [^{11}C]**2** rapidly enters the CNS and shows a relatively high uptake compared to some other tissues that have been sampled. Although the first evidence of the presence of the H_4R in the CNS was conflicting and limited to RT-PCR experiments, more recent studies with immunohistochemical staining and immunoblotting techniques have confirmed the expression of functional H_4R in rat cortex.[10,11,12,14] The distribution of [^{11}C]**2** throughout the CNS appears to be homogeneous at 5 minutes after injection with tracer but after 30 and 60 minutes significant retention of [^{11}C]**2** in the olfactory bulb can be seen that eventually leads to a 2.4-fold higher concentration when compared to the cerebellum (Figure 7). The uptake in the hippocampus shows a similar but less pronounced trend towards retention, whereas the other brain areas contain levels of tracer that are comparable to the cerebellum. Literature has reported **2** to be selective over a broad panel of biological targets and to have an approximately 1000-fold selectivity over the other

histamine receptor subtypes.[6] It is therefore tempting to ascribe the observed retention to the presence of H_4R in olfactory bulb and hippocampus tissue. Future displacement studies with other selective H_4R ligands will have to resolve this issue. Nevertheless, this study clearly demonstrates the ability of [^{11}C]**2** to rapidly cross the blood-brain barrier (BBB) after intravenous injection, whereas [^{11}C]**1** largely remains in the periphery. It has been described that BBB passage is often correlated with polar surface area, a physicochemical property of the ligands that describe the amount of surface in a molecule that is considered as polar.[25] The calculated topological polar surface area (TPSA) of 105.65 Å^2 for compound **1** (Table 1) can be considered high, since it is close to the cut-off value of 120 Å^2 for orally active drugs. A TPSA > 120 Å^2 is considered to make it very unlikely that compounds will be able to pass membranes by passive diffusion.[25,26] The inability of [^{11}C]**1** to cross the blood-brain barrier by passive diffusion is in correspondence with the low permeability value found for this compound in a permeability assay with human TC7 intestinal epithelial cells (Table 1). In order to achieve high brain-penetration, the TPSA is suggested to not exceed the range of 60-70 Å^2.[27] The TPSA calculated for JNJ7777120 is 37.0 Å. This value is well below the suggested range of 60-70 Å and is in accordance with the brain penetration that has been observed in this experiment. The difference in CNS penetration between [^{11}C]**1** and [^{11}C]**2** may be exploited for *in vivo* studies to differentiate between H_4R mediated effects originating in the CNS or in the periphery.

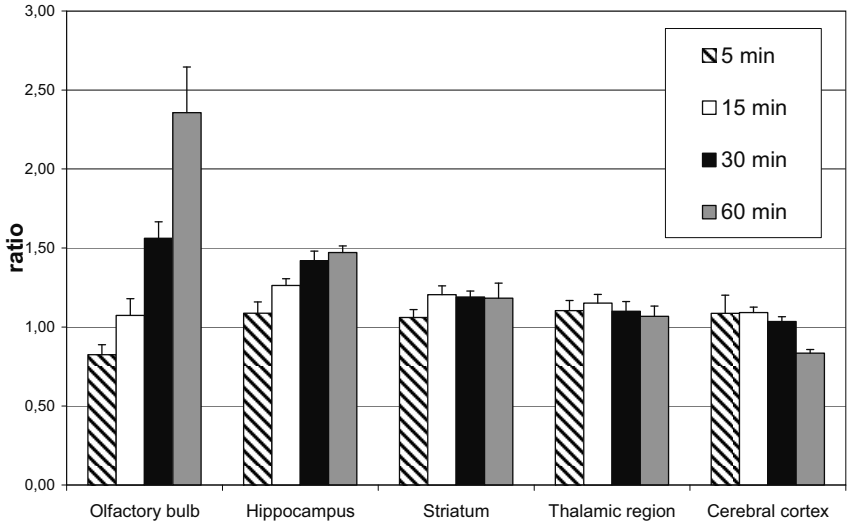

Figure 7: Distribution of [^{11}C]**2** in various brain regions. Ratios of the percentage injected dose/gram for each brain region are determined relative to the cerebellum (arbitrarily set at 1).

Table 1: Physicochemical properties and *in vitro* pharmacology of **1**.

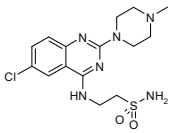

TPSA ($Å^2$)[b]	105.65
A-B permeability (cm/s)[a]	$0.4 * 10^{-6}$
logD (o/w)	1.58
Solubility (μM)	>200

[a] Determined by Cerep (Le Bois l'Evêque, France) using human TC7 cells. [b] Calculated with Molecular Operating Environment (Chemical Computing Group, Montreal, Canada)

Compound **1** was also studied at the human histamine H_1-H_3 receptor subtypes and at the rat and mouse H_4R (Table 2). The selectivity of **1** for the hH_4R over the hH_1R is more than 1000-fold and low displacement of radioligand was found at the hH_2R suggesting good selectivity over the hH_2R as well. The displacement of radioligand at the hH_3R was considerable and may pose a potential selectivity problem when using this ligand as an imaging tool. The affinity for the rH_4R was surprisingly low, whereas the affinity for the mH_4R was high and in the same range as the human H_4R. Such considerable H_4R species differences have been reported previously for a series of other H_4R ligands.[28] It underlines the importance of thorough pharmacological profiling of compounds that are used in *in vivo* studies to be able to understand the observed physiological effects. In this case the affinity of **1** for the rH_4R is considered too low to be used for imaging with PET in rat models. It should be noted that quinazoline **1** has been found to have anti-inflammatory properties *in vivo* and therefore is useful for use in rat models of inflammatory disease. For the optimal use of [^{11}C]**1** in PET-imaging studies the animal of choice should be the mouse, since a pK_i of 8.26 at the mH_4R can be considered good enough for this application. However, even with the current state of the art, delineation of small brain regions or small areas of interest in the periphery is very tedious in mice, thus reducing the possibility to apply mouse models in PET imaging.

In contrast to compound **1**, there are no significant species differences found for **2** amongst the human, mouse and rat H_4R receptors (Table 2).[6] The radioligand of choice for PET-imaging studies in the rat should therefore be [^{11}C]**2**. However, it should be noted that the reference antagonist JNJ7777120 (**2**) is reported to behave as antagonist, but in our hands and in the assays we have used, it displays partial agonism at human, rat and mouse H_4Rs (Table 2).

Table 2: Affinity and functional profile of compound **1** and **2** at different histamine receptors.

	1			**2**		
Receptor	$pK_i \pm SEM$[a]	$pEC_{50} \pm SEM$[b]	α[c]	$pK_i \pm SEM$	$pA_2 \pm SEM$	α
hH_1	5.00 ± 0.10	-	-	<5 [d]	<6 [d]	-
hH_2	27%[f]	-	-	-	<4.5 [d]	-
hH_3	73%[f]	-	-	5.29[d]	<6 [d]	-
hH_4	8.35 ± 0.05	8.00 ± 0.15	-1.64	8.31 ± 0.08	8.04 ± 0.28	0.19
rH_4	7.00 ± 0.10[e]	7.62 ± 0.10	-0.87	8.35 ± 0.10	7.80 ± 0.23	0.57
mH_4	8.26 ± 0.08	6.71 ± 0.11	-0.45	8.40 ± 0.04	7.93 ± 0.23	0.24

[a] Measured by displacement of radioligand binding using previously described methods from literature.[29,30] pK_i's are calculated from at least three independent measurements as the mean ± SEM. [b] Determined in a CRE-ß-glactosidase driven reportergene assay described in literature.[21] [c]α values for agonists have been determined relative to histamine and for inverse agonists relative to thioperamide. [d] Values for compound **2** have been taken from Thurmond *et al.*[6] [e] n=2. [f] Percentage displacement of radioligand at a ligand concentration of 10 μM.

In conclusion, two potent histamine H_4 receptor radioligands suitable for PET studies have been prepared and evaluated in a biodistribution study in rats. Compound [^{11}C]**2** was found to quickly pass the blood-brain barrier, whereas [^{11}C]**1** was only found in the CNS at extremely low concentrations. The inability of [^{11}C]**1** to enter the CNS makes this compound an interesting pharmacological tool that is devoid of CNS effects. Interestingly, [^{11}C]**2** displayed significant retention in olfactory bulb and hippocampus tissue, suggesting the presence of H_4R in these brain regions. The possible presence of the H_4R in discrete brain regions warrants further research into the exact location and relevance of the H_4R in the CNS.

Experimentals

All chemicals were purchased from commercial suppliers unless mentioned otherwise. The saline phosphate buffer, sterile water and ethanol used for formulation of the final product were purchased from the VUmc pharmacy. $^{11}CO_2$ was produced with an IBA 18/9 Cyclone cyclotron.[31] The semi-automated radiosynthesis was performed in customized apparatus including the preparative HPLC system that consists of a Jasco PU-1587 HPLC pump, a six-way VICI injector (VA EPC6W) with a 5-ml loop, an Xterra PrepMS (C18)5µ column (100 mm x 30 mm), a Jasco UV1575 UV detector and a Na(I) radioactivity detector. The radioactivity of the formulated products was measured with a Veenstra VDC-405 dosis calibrator.

Analytical HPLC analyses were conducted using a Jasco PU-1580 HPLC pump, a Rheodyne injector with a 100-µl loop, an Xbridge™ (C18) 5µ column (100 mm x 4.6 mm) using a flow of 1.0 ml/min., with a Jasco UV2075 UV detector operating at 225 nm. A mixture of 20% MeCN-80% water containing 0.1% diisopropylethylamine was used for analysis of [^{11}C]**1** and 30% MeCN-70% water containing 0.1% diisopropylethylamine was used for analysis of [^{11}C]**2** .

Radiosynthesis and formulation of [^{11}C]1.

Freshly prepared [^{11}C]CH_3I (16-20 GBq) was transferred to a reaction vial containing a solution of the dihydrochloride salt of (**5**) (2.0 mg, 4.4 µmol) in a mixture of DMF (0.3 ml), MeCN (0.2 ml), water (0.1 ml) and DIPEA (5.0 µl). After heating at 70 °C for 5 minutes the reaction mixture was cooled to room temperature and purified by preparative HPLC at a flow of 20 ml/min (Figure 2). The collected fraction containing the desired compound was diluted with water for injection (60 ml) and the resulting solution was passed over an SPE (solid phase extraction) column (Sep-Pak tC18). The SPE column was washed with water for injections (20 ml) and eluted with ethanol (96%, 1.0 ml) and phosphate buffered saline (9.0 ml of 7.1 mM NaH_2PO_4 in 0.9% NaCl with 0.4% polysorbatum-80), to give the product in a sterile, isotonic and pyrogen free solution. The final formulation contained 1776±373 MBq of [^{11}C]VUF10558 (40%, decay corrected yield). The identity of the radioligand was confirmed by analytical HPLC of a sample of radioligand spiked with cold **2**. Radiochemical purities were typically larger than 99% as determined by analytical HPLC. The specific activity was between 20 and 40 GBq/µmol.

Radiosynthesis and formulation of [^{11}C]2.

Freshly prepared [^{11}C]CH_3I (16-20 GBq) was transferred to a reaction vial containing a solution of **9** (1.0 mg, 3.8 µmol) in MeCN (0.5 ml). After heating at 70 °C for 5 minutes the reaction mixture was cooled to room temperature and purified by preparative HPLC at a flow of 20 ml/min (Figure 3). The fraction containing the desired compound was diluted with water for injections (60 ml) and the resulting solution was passed over an SPE column (Sep-Pak tC18). The SPE column was washed with water for injections (20 ml) and eluted with ethanol (96%, 1.0 ml) and phosphate buffered saline (9.0 ml of 7.1 mM NaH_2PO_4 in 0.9% NaCl with 0.4% polysorbatum-80). The final formulation contained 1700±267 MBq of [^{11}C]**2** (40 % decay corrected yield). The identity of the radioligand was confirmed by analytical HPLC of a sample of radioligand spiked with **2**. Radiochemical purities were typically larger than 99% as determined by analytical HPLC. The specific activity was between 20 and 40 GBq/µmol.

Biodistribution study of [^{11}C]1 and [^{11}C]2 in rats

[^{11}C]**1** or [^{11}C]**2** (approximately 50 MBq) were injected intravenously into male Wistar rats (200-250 g) anaesthetized with isoflurane. The animals were sacrificed under anesthesia at

5, 15, 30 and 60 minutes post injection by cervical dislocation. A blood sample was taken by cardiac puncture and plasma was collected after centrifugation. The animals were dissected rapidly and the selected tissues were collected and weighed. Residual radioactivity in the tissues was measured with an LKB Wallac 1282 compugamma CS and expressed as percentage of injected dose per gram of tissue (%ID/g). All animal studies were performed with the approval of the animal ethics committee of VU University Amsterdam.

Pharmacological and physicochemical profiling of 1

The hH_1R and hH_4R affinities have been determined according to previously described methods.[23,24] Single point radioligand displacement studies at the hH_2R and hH_3R were performed in duplo by Cerep (Le Bois l'Evêque, France). Functional behavior at the human H_4R (hH_4R), rat H_4R (rH_4R) and mouse H_4R (mH_4R) was determined using a method that has been reported in literature[21] logD and membrane passage parameters were determined by Cerep (Le Bois l'Evêque, France).

Synthesis of precursors for [^{11}C] labeled (5-chloro-1*H*-2-yl)(4-methylpiperazin-1-yl)methanone, 1 ([^{11}C]VUF10558) and.2-(6-chloro-2-(4-methylpiperazin-1-yl)quinazoline-4-amino)-ethanesulfonamide, 2 ([^{11}C]JNJ7777120)

2-(6-chloro-2-(4-tert-butylcarboxylate-piperazin-1-yl)quinazoline-4-amino)-ethanesulfonamide (4)

To a solution of 2,4,6-trichloroquinazoline (**3**) (200 mg, 0.86 mmol) and DIPEA (0.40 ml) in THF (3.0 ml) was added 2-aminoethanesulfonamide hydrochloride (138 mg, 0.86 mmol) and the resulting suspension was stirred until conversion was completed (monitored by TLC). The product was reacted without purification with boc-piperazine (320 mg, 1.72 mmol) and the reaction mixture was heated at 160 °C for 10 minutes under microwave irradiation. After cooling to room temperature the mixture was diluted with EtOAc and washed with water and brine. Removal of the organic phase gave the crude product which was recrystallized from EtOAc/MeOH to yield 95 mg (20%) of white crystals. ^{1}H NMR (CD_3OD) δ (ppm) 7.85 (d, J= 2.3 Hz, 1H), 7.49 (dd, J= 2.3 Hz, J= 9.0 Hz, 1H), 7.35 (d, J= 9.0 Hz, 1H), 4.04-3.97 (m, 2H), 3.89-3.84 (m, 4H), 3.52-3.43 (m, 6H), 1.46 (s, 9H).

2-(6-chloro-2-(piperazin-1-yl)quinazoline-4-amino)-ethanesulfonamide dihydrochloride (5)

a solution of 4 M HCl in dioxane (1.0 ml) was added to 2-(6-chloro-2-(4-tert-butylcarboxylate-piperazin-1-yl)quinazoline-4-amino)-ethanesulfonamide (**4**, 250 mg, 0.53 mmol) in dioxane (3.0 ml) and the resulting mixture was stirred at room temperature. After 16 hours, the obtained suspension was evaporated to dryness and the white residue was recrystallized from EtOH/water to yield 130 mg (55%) of a white solid. ^{1}H NMR (CD_3OD) δ (ppm) 7.63 (d, J= 1.9 Hz, 1H), 7.42 (d, J= 8.8 Hz, 1H), 7.20 (dd, J= 1.9 Hz, J= 8.8 Hz, 1H), 6.88 (s, 1H), 4.10 (t, J=5.3 Hz, 4H), 3.35 (t, J=5.3 Hz, 4H).

tert-butyl 4-(5-chloro-1*H*-indole-2-carbonyl)piperazine-1-carboxylate (8)

This compound was prepared according to a procedure described in literature.[23] Yield 369 mg (40%). ^{1}H NMR (DMSO-δ_6) δ (ppm) 11.83 (br s, 1H), 7.67 (d, J= 1.9 Hz, 1H), 7.43 (d, J= 8.7 Hz, 1H), 7.20 (dd, J=8.7 Hz, J=1.9 Hz, 1H), 6.83 (s, 1H), 3.74 (m, 4H), 3.47-3.44 (m, 4H), 1.44 (s, 9H).

(5-chloro-1*H*-indol-2-yl)(piperazin-1-yl)methanone (9)
To a solution of *tert*-butyl 4-(5-chloro-1*H*-indole-2-carbonyl)piperazine-1-carboxylate (200 mg,) in dioxane (2 ml) was added a solution of 4M HCl in dioxane (2.0 ml) and the resulting mixture was stirred at room temperature until TLC indicated complete conversion of the starting material. The solvent was removed under reduced pressure and the residual solid was partitioned between a layer of saturated $NaHCO_3$ and EtOAc. The aqueous phase was extracted thoroughly with EtOAc and the combined organic phases were dried over Na_2SO_4. Removal of the solvent yielded 146 mg (73%) of the title compound as a white solid. ^{1}H NMR (DMSO-δ_6) δ (ppm) 11.80 (br s, 1H), 7.66 (d, *J*= 2.0 Hz, 1H), 7.43 (d, *J*= 8.7 Hz, 1H), 7.19 (dd, *J*= 2.0 Hz, *J*= 8.7 Hz, 1H), 6.75 (s, 1H), 3.66 (m, 4H), 2.52 (t, *J*= 4.9 Hz, 4H).

Acknowledgements
The authors gratefully acknowledge the BV cyclotron for the production of $^{11}CO_2$. Thanks also goes out to Koos Herscheid, Joost Verbeek, Hans Buiter and Rob Klok for assistance in the biodistribution experiments.

References

[1] Oda, T.; Morikawa, N.; Saito, Y.; Masuho, Y.; Matsumoto, S. Molecular cloning and characterization of a novel type of histamine receptor preferentially expressed in leukocytes. *J. Biol. Chem.* **2000**, 275:36781-86.

[2] Taglialatela, M.; Castaldo, P.; Pannaccione, A.; Secondo, M.; Cataldi, F.; Boscia, F.; Annunziato, L. First- and second-generation H_1 antihistamines: from their molecular basis of their interaction with HERG K^+ channels to physiological and pathophysiological implication. *Clin. Exp. All. Rev.* **2004**, 4:183-190.

[3] Shin, J., M.; Vagin, O.; Munson, K.; Kidd, M.; Odlin, I., M.; Sachs, G. Molecular mechanisms in therapy of acid-related diseases. *Cell. Mol. Life Sci.* **2008**, 65:264-81.

[4] Wijtmans, M.; Leurs, R.; de Esch, I., J., P. Histamine H_3 receptor ligands break ground in a remarkable plethora of therapeutic areas. *Exp. Opin. Invest. Drugs.* **2007**, 16:967-85.

[5] Coruzzi, G.; Adami, M.; Guaita, E.; de Esch, I.J.P.; Leurs, R. Antiinflammatory and antinociceptive effects of the selective histamine H_4-receptor antagonists JNJ7777120 and VUF6002 in a rat model of carrageenan-induced inflammation. *Eur. J. Pharmacol.* **2007**, 563;240-44.

[6] Thurmond, R., L.; Desai, P., J.; Dunford, P., J.; Fung-Leung, W., P.; Hofstra, C., L.; Jiang, W.; Nguyen, S.; Riley, J., P.; Sun, S.; Williams, K., N.; Edwards, J., P.; Karlsson, L. A potent and selective histamine H_4 receptor antagonist with anti-inflammatory properties. *J. Pharmacol. Exp. Ther.* **2004**, 309:404-13.

[7] Takeshita, K.; Sakai, K. l.; Bacon, K., B.; Ganter, F. Critical role of L-selectin and histamine H4 receptor in zymosan-induced neutrophil recruitment from the bone marrow: comparison with carrageenan. *J. Pharmacol. Exp. Ther.* **2004**, 310:272-80.

[8] Ikawa, Y.; Suzuki, M.; Shiono, S.; Ohki, E.; Moriya, H.; Negishi, E.; Ueno, K. Histamine H_4 receptor expression in human synovial cells obtained from patients suffering from rheumatoid arthritis. *Biol. Pharm. Bull.* **2005**, 28:2016-18.

[9] Morse, K.l.; Behan, J.; Laz, T.M.; West, R.E. Jr.; Greenfender, S.A.; Anthes, J.C.; Umland, S.; Wan, Y.; Hipkin, R.W.; Gonsiorek, W.; Shin, N.; Gustafson, E.L.; Qiao, X.; Wang, S.; Hedrick, J.A.; Green, J.; Bayne, M.; Monsma, F.J. Jr.; Cloning and characterization of a novel human histamine receptor. J. Pharmacol. Exp. Ther. **2001**, 296:1058-66.

[10] Coge, F.; Guenin, S., P.; Rique, H.; Boutin, J., A.; Galizzi, J., P. Structure and expression of the human histamine H_4-receptor gene. Biochem. Biophys. Res. Commun. **2001**, 284:301-09.

[11] Nakamura, T.; Itadani, H.; Hidaka, Y.; Ohta, M.; Tanaka, K. Molecular cloning and characterization of a new human histamine receptor, HH_4R. *Biochem. Biophys. Res. Commun.* **2000**, 279:615-20.

[12] Dijkstra, D.; Leurs, R.; Chazot, P.; Shenton, F., C. ; Stark, H. ; Werfel, T.; Gutzmer, R. Histamine downregulates monocyte CCL2 production through the histamine H_4 receptor. **2008** *J. Allergy Clin. Immunol.* 120;300-7.

[13] Sander, L., E; Lorentz, A.; Sellge, G.; Coeffier, M.; Neipp, M.; Veres, T.; Frieling, T.; Meier, P., N.; Manns, M., P.; Bischoff, S., C. Selective expression of histamine receptors H_1R, H_2R and H_4R, but not H_3R, in the human intestinal tract. *Gut.* **2006**, 55:498-504.

[14] Chazot, P.; Connelly, W.; Shenton, F., C.; Lethbridge, N.; van Rensburg, R.; Lees, R. Further evidence for H_4 histamine receptor expression on central neurons. EHRS XXXVIIth annual meeting 7th-10th May 2008, Stockholm, Sweden.

[15] Gutzmer, R.; Diestel, C.; Mommert, S.; Kother, B.; Stark, H.; Wittmann, M.; Werfel, T. Histamine H_4 receptor stimulation suppresses IL-12p70 production and mediates chemotaxis in human monocyte-derived dendritic cells. *J. Immunol.* **2005**, 174:5224-32.

[16] Ling, P.; Ngo, K.; Nguyen, S.; Thurmond, R., L.; Edwards, J., P.; Karlsson, L.; Fung-Leung, W., P. Histamine H_4 receptor mediates eosinophil chemotaxis with cell shape change and adhesion molecule upregulation. *Br. J. Pharmacol.***2004**, 142:161-171.

[17] Lammertsma, A., A. Radioligand studies: imaging and quantitative analysis. *Eur. Neuropsychopharmacology.* **2002**, 12:513-16.

[18] Smits, R., A.; Istyastono, E., P. ; Zuiderveld, O., P.; van Dam, C., M.; de Kanter, F. ; Jongejan, A.; Coruzzi, G.; Adami, M.; Leurs, R.; de Esch, I., J., P. Synthesis and QSAR of quinazoline sulfonamides as highly potent human histamine H_4 receptor inverse agonists. *Manuscript in preparation.*

[19] Venable, J., D.; Cai, H.; Chai, W.; Dvorak. C., A.; Grice, C., A.; Jablonowski, J. A.; Shah, C., R.; Kwok, A., K.; Ly, K., S.; Pio, B.; Wei, J.; Desai, P., J;. Jiang, W.; Nguyen, S.; Ling, P.; Wilson, S., J.; Dunford, P., J.; Thurmond, R., L.; Lovenberg, T., W.; Karlsson, L.; Carruthers, N., I.; Edwards, J., P. Preparation and biological evaluation of indole, benzimidazole, and thienopyrrole piperazine carboxamides: potent human histamine h(4) antagonists. *J. Med. Chem.* **2005**, 48:8289-98.

[20] Crouzel, C. ; Langstrom, B. ; Pike, V., W.; Coenen, H., H. *Applied radiation and isotopes.* **1987**, 38 :601-603.

[21] Smits, R., A.; de Esch I., J., P.; Zuiderveld, O., P.; Broeker, J.; Sansuk, K.; Guaita, E.; Coruzzi, G.; Adami, M.; Haaksma, E.; Leurs, R. The discovery of quinazolines as histamine H_4 receptor inverse agonists using a scaffold hopping approach. Submitted to *J. Med. Chem.*

[22] Miller, E.; Sprague, J., M.; Kissinger, L., W.; McBurney, L., F. The preparation of some amino sulfonamides. *J. Am. Chem. Soc.* **1940**, 62:2099-2103.

[23] Jablonowski, J.A.; Grice, C.A.; Dvorak, C.A.; Venable, J.D.; Kwok, A.K.; Ly, K.S.; Wei, J.; Baker, S.M.; Desai, P.J.; Jiang, W.; Wilson, S.J.; Thurmond, R.L.; Karlsson, L.; Edwards, J.P.; Lovenberg, T.W.; Carruthers, N.I. The first potent and selective non-imidazole human histamine H_4 receptor antagonists. *J. Med. Chem.* **2003** 19:3957-60.

[24] Airaksinen, A., J.; Jablonowski, J., A.; van der Mey, M.; Barbier, A., J.; Klok, R., P.; Verbeek, J.; Schuit, R.; Herscheid, J., D., M.; Leysen, J., E.; Carruthers, N., I.; Lammertsma, A., A.; Windhorst, A., D. Radiosynthesis and biodistribution of a histamine H_3 receptor antagonist 4-[3-(piperidin-1-yl-but-1-ynyl)-[^{11}C]benzyl]-morpholine: evaluation of a potential PET ligand. *Nucl. Med. Biol.* **2006**, 801-10.

[25] Ertl, P.; Rohde, B.; Selzer, P. Fast calculation of molecular polar surface area as a sum of fragment-based contributions and ist application to the prediction of drug transport properties. *J. Med. Chem.* **2000,** 43:3712-17.

[26] Bohets, H.; Annaert, P.; Mannens, G.; van Beijsterveldt, L.; Anciaux, K.; Verboven, P.; Meuldermans, W.; Lavrijsen. K. Strategies for absorption screening in drug discovery and development. *Curr. Top. Med. Chem.* **2001**, 1:367:83.

[27] Kelder, J.; Grootenhuis, P., D.; Bayada, D., M.; Delbressine, L., P.; Ploemen, J., P. Polar molecular surface as a dominating determinant for oral absorption and brain penetration of drugs. *Pharm. Res.* **1999**, 16:1514-9.

[28] Liu, C.; Wilson, S., J.; Kuei, C.; Lovenberg, T., W. Comparison of human, mouse, rat, and guinea pig histamine H_4 receptors reveals substantial pharmacological species variation. *J. Pharmacol. Exp. Ther.* **2001**, 299:121-30.

[29] Bakker, R.A.; Weiner, D., M.; ter Laak, T.; Beuming, T.; Zuiderveld, O., P.; Edelbroek, M.; Hacksell, U.; Timmerman, H.; Brann, M., R.; Leurs, R. 8R-lisuride is a potent stereospecific histamine H1-receptor partial agonist. *Mol. Pharmacol.* **2004**, 65:538-49.

[30] Smits, R., A.; Lim, H., D.; Hanzer, A.; Zuiderveld, O., P.; Guaita, E.; Adami, M.; Coruzzi, G.; Leurs, R.; de Esch I., J., P. Fragment based design of new H_4 receptor-ligands with anti-inflammatory properties in vivo. *J. Med. Chem.* **2008**, 51:2457-67.

[31] Luurtsema, G.; Windhorst, A., D.; Mooijer, M., P., J.; Herscheid, J., D., M.; Lammertsma, A., A.; Franssen, E., J., F.; Fully automated high yield synthesis of (*R*)- and (*S*)-[^{11}C]verapamil for measuring P-glycoprotein function with positron emission tomography. *J. Label. Compd. Radiopharm.* **2002**, 45:1199-1207.